BIOCHEMISTRY
including biophysical chemistry & molecular biology

Article

pubs.acs.org/biochemistry

A Ferric–Peroxo Intermediate in the Oxidation of Heme by IsdI

Shin-ichi J. Takayama,[†,‡,§] Slade A. Loutet,[†] A. Grant Mauk,[‡,§] and Michael E. P. Murphy*[,†]

[†]Department of Microbiology and Immunology, [‡]Department of Biochemistry and Molecular Biology, and [§]UBC Centre for Blood Research, University of British Columbia, Vancouver, British Columbia V6T 1Z3, Canada

ABSTRACT: The canonical heme oxygenases (HOs) catalyze heme oxidation via a heme-bound hydroperoxo intermediate that is stabilized by a water cluster at the active site of the enzyme. In contrast, the hydrophobic active site of IsdI, a heme-degrading enzyme from *Staphylococcus aureus*, lacks a water cluster and is expected to oxidize heme by an alternative mechanism. Reaction of the IsdI–heme complex with either H_2O_2 or *m*-chloroperoxybenzoic acid fails to produce a specific oxidized heme iron intermediate, suggesting that ferric–hydroperoxo or ferryl derivatives of IsdI are not involved in the catalytic mechanism of this enzyme. IsdI lacks a proton-donating group in the distal heme pocket, so the possible involvement of a ferric–peroxo intermediate has been evaluated. Density functional theory (DFT) calculations indicate that heme oxidation involving a ferric–peroxo intermediate is energetically accessible, whereas the energy barrier for a reaction involving a ferric–hydroperoxo intermediate is too great in the absence of a proton donor. We propose that IsdI catalyzes heme oxidation through nucleophilic attack by the heme-bound peroxo species. This proposal is consistent with our previous demonstration by nuclear magnetic resonance spectroscopy that heme ruffling increases the susceptibility of the *meso*-carbon of heme to nucleophilic attack.

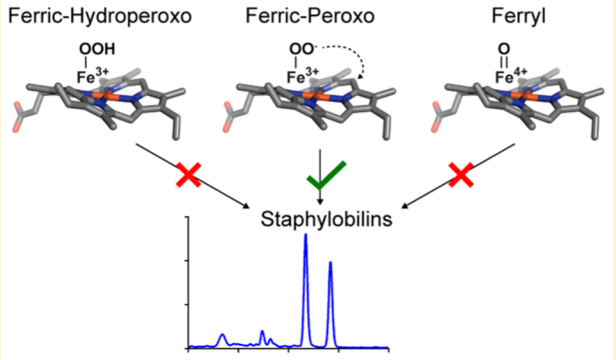

Acquisition of iron from the extracellular environment is an essential function of pathogenic bacteria.[1] The Gram-positive bacterium *Staphylococcus aureus* is a common nosocomial and community-acquired, multidrug resistant pathogen[2] that employs several mechanisms to acquire iron from a host, including the acquisition of heme from host heme-containing proteins.[3] Following the acquisition of heme, *S. aureus* uses the paralogous cytoplasmic proteins, IsdG and IsdI, to degrade heme and release iron.[4]

Enzymatic oxidation of heme is a complex, multistep process that is achieved by at least two different mechanistic processes. Canonical heme oxygenases (HOs) initially form a hydroperoxo [Fe(III)–OOH] intermediate that facilitates oxidation of the heme *α-meso*-carbon to form *α-meso*-hydroxyheme.[5−9] This intermediate then proceeds to formation of biliverdin and carbon monoxide (Figure 1).[10] The HO active site contains a network of ordered water molecules[11,12] that donate a proton to a coordinated dioxygen to form the Fe(III)–OOH intermediate.[13,14] On the other hand, *S. aureus* IsdG and IsdI catalyze oxidation of heme to roughly equimolar amounts of two novel tetrapyrroles, 5-oxo-*δ*-bilirubin and 15-oxo-*β*-bilirubin (collectively known as staphylobilins)[15] with concomitant production of formaldehyde (Figure 1).[16] Formation of these products is supported *in vitro* with the addition of either the chemical reductant ascorbic acid[15] or NADPH-IruO, the proposed physiological reductase.[17] IsdG and IsdI exhibit two significant structural differences from the classical heme oxygenases that presumably account for the differences in their products. First, the active sites of IsdG and IsdI lack the cluster of water molecules[18,21] that donates a proton required to form an Fe(III)–OOH intermediate. Second, binding of heme to the active site of either IsdG or IsdI results in significant ruffling of the heme structure as demonstrated by the X-ray crystal structures of the heme-bound forms of these proteins.[15,18,19] Nuclear magnetic resonance (NMR) experiments suggest that this ruffling renders the heme *meso*-carbons more susceptible to nucleophilic attack than is the case for nearly planar heme bound to canonical HOs.[20−22] Active site amino acid substitutions of IsdI that reduce the extent of heme ruffling also impair heme degradation.[19]

In addition to the hydroperoxide species used by HO, other reactive iron oxide species have been described for heme-containing oxygenase enzymes. For example, the monooxygenase activity of many cytochrome P450 proteins involves an intermediate known as compound I that possesses a ferryl species [Fe(IV)=O] and a heme cation radical,[23] though there is continuing debate concerning the protonation state of the ferryl oxygen. Fe–O bond lengths determined through X-ray crystallography, extended X-ray absorption spectroscopy, and resonance Raman spectroscopy indicate that the oxygen is deprotonated for the ferryl forms of many enzymes.[24] Mössbauer spectroscopy and DFT calculations for CYP101 and CYP102A1 suggest that for theses enzymes, the ferryl center of compound I is protonated at physiological pH.[25]

Received: March 5, 2015
Revised: April 8, 2015
Published: April 8, 2015

DOI: 10.1021/acs.biochem.5b00239
Biochemistry 2015, 54, 2613−2621

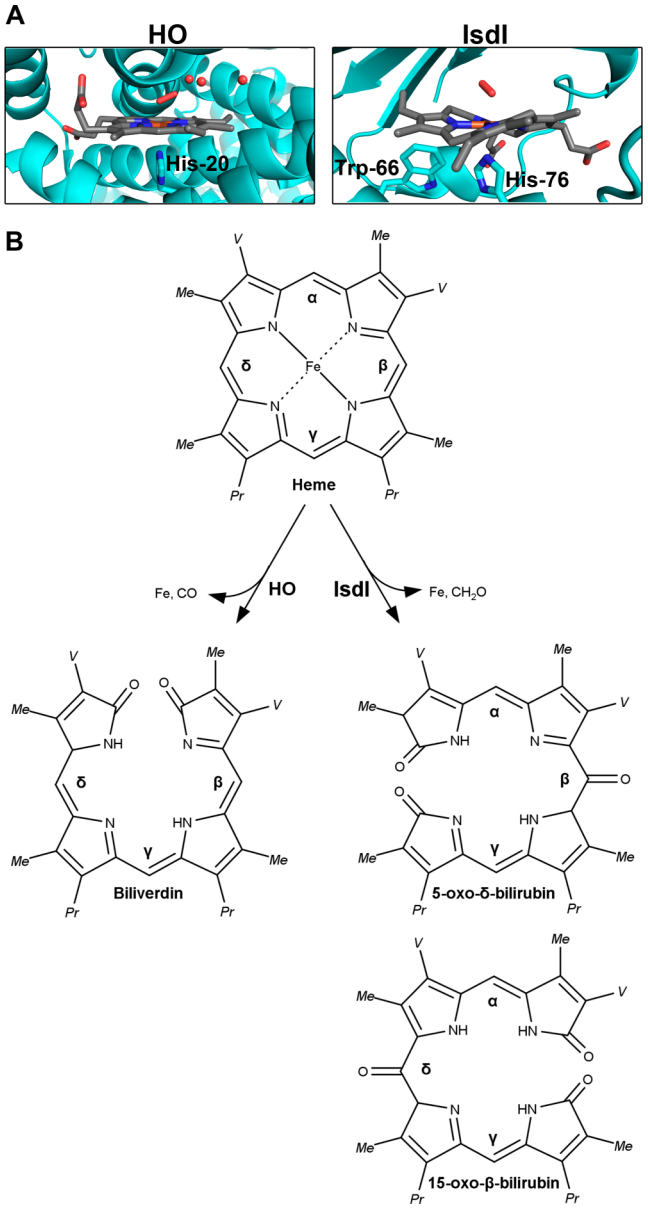

Figure 1. (A) Active sites and (B) heme degradation products of canonical HOs and IsdI. (A) HO and IsdI active site images were generated with PyMOL[56] from PDB entries 1V8X[11] and 3LGN,[15] respectively. In both cases, a histidine residue coordinates the iron atom, while in IsdI, a tryptophan at position 66 contributes to heme ruffling. In HO, the water nearest the dioxygen molecule is ~2.5 Å away, while in IsdI, the nearest water is >7 Å away and is located on the opposite side of the heme group. Carbons in the protein and heme are colored cyan and gray, respectively. Nitrogen (dark blue), oxygen (red), and iron (brown) are shown in the colors indicated, and waters are displayed as red spheres. (B) Chemical structures were generated using MarvinSketch (version 14.12.8.0). For the sake of simplicity, the ring substituents of heme, biliverdin, 5-oxo-*δ*-bilirubin, and 15-oxo-*β*-bilirubin are drawn as *Me* (methyl), *V* (vinyl), and *Pr* (propionate).

Recently, cryocrystallography using neutron diffraction showed more directly that the ferryl oxygen of cytochrome *c* peroxidase compound ES (an analogue of compound I in which the radical resides on an amino acid residue) is unprotonated.[26] For these proteins, an additional ferryl intermediate, compound II [Fe(IV)−OH], that lacks the cation radical also exists.[27]

Some cytochromes P450 (e.g., CYP17,[28] CYP19,[29] CYP51,[30] and CYP125[31]) use a ferric−peroxo [Fe(III)−OO^-] species for nucleophilic addition of oxygen to aldehydes. The dioxygenases indolamine 2,3-dioxygenase (IDO) and tryptophan 2,3-dioxygenase (TDO) open the pyrrole rings of indoleamines such as tryptophan and insert both atoms of dioxygen into the resulting product by means of a ferric−superoxo [Fe(III)−$OO^{\bullet-}$] species; however, this species rarely serves as a catalytic intermediate among heme-containing oxygenases.[32]

In this study, we use a combination of spectroscopy, chromatography, and DFT calculations to show that, unlike HO, the first step in heme oxidation by IsdI is unlikely to involve an Fe(III)−OOH intermediate but likely proceeds via a ferric−peroxo [Fe(III)−OO^-] intermediate and a nucleophilic attack pathway.

EXPERIMENTAL PROCEDURES

Sample Preparation. Recombinant IsdI was expressed, purified, and reconstituted with heme as reported previously.[4,18]

Electronic Absorption Spectroscopy. The electronic absorption spectra (20 °C) of IsdI (~10 μM) in Tris-HCl buffer (20 mM, pH 7.4, with 100 mM NaCl) were recorded with a Cary model 6000i spectrophotometer (Varian Inc.) equipped with a Peltier thermoregulator. Activity assays were initiated by the addition of peroxides, and spectra were recorded at 1 min intervals. Reactions in the presence of excess (2 mM) guaiacol were performed in the same buffer. To permit approximate quantitative comparison of rates of reactions reported here, changes in Soret peak (412 nm) intensity were fit by nonlinear regression to a single-exponential function with GraphPad Prism version 6.00 to produce apparent first-order rate constants (k^{app}). While all of these fits to kinetic data exhibited R^2 of >0.97, we attribute no mechanistic significance to them.

Analysis of Reaction Products. Enzymatic assays were performed with solutions of 100 μM IsdI−heme complex in 50 mM Tris-HCl (pH 7.4) and 100 mM NaCl (300 μL). Heme degradation was initiated with 2 mM ascorbic acid, or various concentrations of H_2O_2 or *m*-chloroperoxybenzoic acid (*m*CPBA). After reactions had reached completion (30−60 min), buffer was removed with a Nanosep centrifugal device (Pall Corp.; pore size of 10 kDa). Protein was resuspended in acetonitrile (50%, 150 μL) containing trifluoroacetic acid (0.1%). Reaction products were separated from the protein with a Nanosep centrifugal device. For experiments with two reaction steps, after the first step the protein was separated from solution and resuspended in fresh buffer, and then ascorbic acid was added. Samples of reaction products were separated by reverse-phase high-performance liquid chromatography (HPLC) (Beckman System Gold) using an Alltech Prosphere HP C_{18} 300A column, equilibrated in a 5% acetonitrile/H_2O solvent containing TFA (0.1%). The column was developed with a gradient (5 to 80% acetonitrile for 20 min at a flow rate of 0.8 mL min^{-1}). ESI-MS analyses of the products were conducted with an Agilent model 6210 liquid chromatography-MS system equipped with an electrospray ion source (capillary voltage, 3 kV; fragmentor voltage, 70 eV) and a quadrupole detector operating in the positive scan mode (*m*/*z* 300−700).

DFT Calculation. All calculations were performed with the B3LYP functional as implemented in Gaussian09.[33] Porphine and imidazole were used as models of heme and His ligands,

DOI: 10.1021/acs.biochem.5b00239
Biochemistry 2015, 54, 2613−2621

respectively. The double-ζ LACVP(Fe)/6-31G(H,C,N,O,S) and LACVP(Fe)/6-31+G*(H,C,N,O,S) basis sets were employed for geometry optimization of Fe(III)−OOH and Fe(III)−OO^- species, respectively. A low-spin doublet state was considered for both species. Vibrational analysis showed that optimized reactant and product structures have no imaginary frequency and transition states have only one imaginary frequency mode that correctly connects a reactant and a product. After optimization, single-point energy calculations were performed with the Wachter's+f basis set[34] for Fe and the 6-311+G** basis set for the remaining atoms. All the energies reported in this paper are the values obtained by single-point calculations with a zero-point energy correction.

RESULTS

Reaction of the IsdI−Heme Complex with H_2O_2. In the case of HO, addition of equimolar H_2O_2 to the heme-bound protein results in an almost stoichiometric yield of verdoheme, which has a characteristic absorption maximum near 700 nm.[35] However, reaction of the IsdI−heme complex with H_2O_2 (1 equiv) decreased the intensity of the Soret maximum by approximately one-third (k^{app} ∼ 0.1 min^{-1}) and produced no observable absorption maximum around 700 nm (Figure 2A).

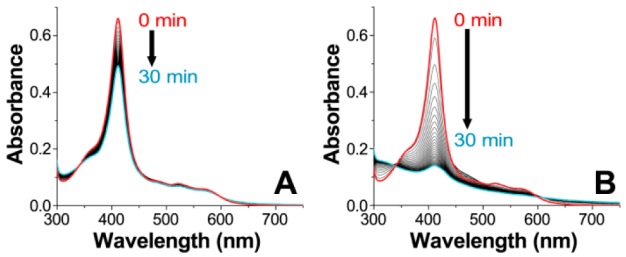

Figure 2. Reaction of the IsdI−heme complex (10 μM) with (A) 10 or (B) 50 μM H_2O_2. Reactions were initiated by the addition of H_2O_2, and electronic absorption spectra were recorded at 1 min intervals for 30 min.

For comparison, degradation of IsdI heme with ascorbic acid as a reductant exhibits a k^{app} of ∼0.066 min^{-1}.[19] Nearly complete loss of the Soret maximum of IsdI was observed in the reaction with excess (5 equiv) H_2O_2 (k^{app} ∼ 0.18 min^{-1}), but again, no band arose at 700 nm (Figure 2B). HPLC analysis of the products of reaction with H_2O_2 (1 equiv) identified only one major product [λ_{max} ∼ 400 nm (Figure 3B)]. The mass of this product as determined by LC-MS was 616.2 Da, which corresponds to the mass of unmodified heme. The intensity of the HPLC peak for unmodified heme was approximately half of that observed following identical analysis of the untreated IsdI−heme complex (Figure 3A,B). No major product was observed by HPLC analysis following reaction of the IsdI−heme complex with 5 equiv of H_2O_2 (Figure 3C). These results indicate that IsdI is not as reactive as HO toward H_2O_2 and that this reaction results primarily in random degradation of heme rather than conversion to a specific intermediate. Addition of ascorbic acid to the protein after reaction of the IsdI−heme complex with H_2O_2 (1 equiv) produced the two staphylobilins, both of which absorb around 460 nm (Figure 4B); however, the yield of staphylobilins was approximately half the amount obtained following reaction with ascorbic acid alone (Figure 4A). Addition of ascorbic acid after reaction with H_2O_2 (5 equiv) did not produce any specific product (Figure 4C). In the presence of heme−ferryl species (e.g., compound I or II),

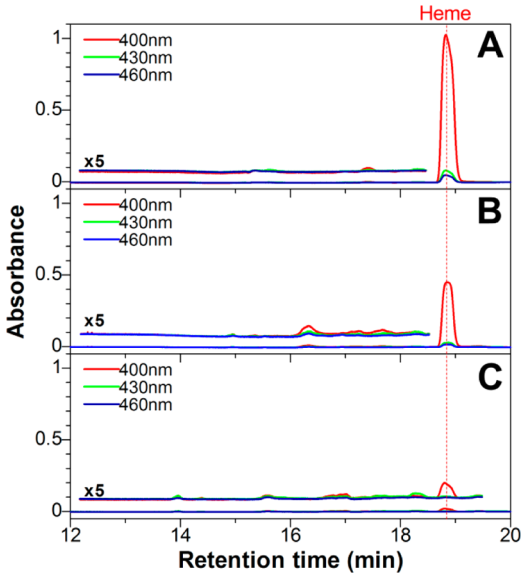

Figure 3. HPLC traces of H_2O_2 reaction products separated with a linear acetonitrile gradient. The IsdI−heme complex (100 μM) was reacted with (A) 0, (B) 100, or (C) 500 μM H_2O_2.

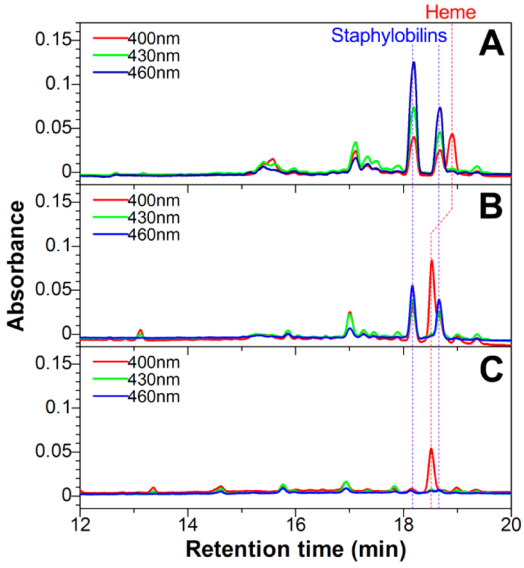

Figure 4. HPLC traces of the products resulting from two-step reactions. The IsdI−heme complex (100 μM) was reacted with (A) 0, (B) 100, or (C) 500 μM H_2O_2 followed by ascorbate (2 mM). The unmodified heme peak appeared at a slightly shifted elution time in panels B and C compared to panel A probably because of heme redox state differences.

guaiacol is oxidized to a tetrameric compound that absorbs at 470 nm.[36] Reactions of the IsdI−heme complex with H_2O_2 (5 equiv) in the presence of excess guaiacol (Figure 5A) (k^{app} ∼ 0.26 min^{-1}) proceeded as in the absence of guaiacol (Figure 2B). No significant increase in absorption around 470 nm was observed, suggesting that ferryl species were not formed during the H_2O_2 reaction.

Reaction of the IsdI−Heme Complex with *m*CPBA. Heme-coordinated acyl hydroperoxides such as *m*-chloroperoxybenzoic acid (*m*CPBA) can cleave heterolytically to produce ferryl−heme intermediates.[23] Indeed, addition of *m*CPBA to the IsdI−heme complex in the presence of guaiacol resulted in

DOI: 10.1021/acs.biochem.5b00239
Biochemistry 2015, 54, 2613−2621

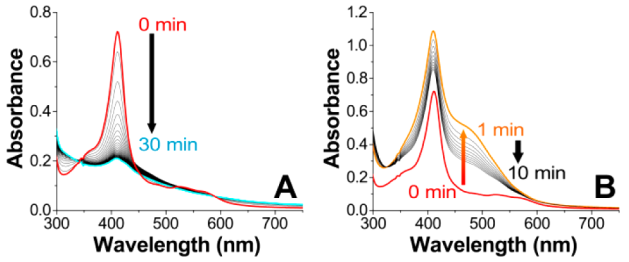

Figure 5. Reaction of the IsdI–heme complex (10 μM) with hydroperoxides (500 μM) in the presence of excess (2 mM) guaiacol. (A) H_2O_2 reaction. Electronic spectra were recorded at 1 min intervals for 30 min. (B) *m*CPBA reaction: red for 0 min and orange for 1 min. Subsequently, spectra were recorded at 1 min intervals for up to 10 min (black).

a rapid increase in absorption around 470 nm (Figure 5B), as expected for the oxidation of guaiacol to tetraguaiacol. After 1 min, absorption at 470 nm began to decrease, but the Soret intensity was unchanged relative to a changing background throughout the reaction ($k^{app} \sim 0.18$ min^{-1}), indicating that the ferryl species produced by the reaction was predominantly consumed by guaiacol oxidation (Figure 5B). In the absence of guaiacol, addition of *m*CPBA (5 equiv) to the IsdI–heme complex slightly decreased the intensity and blue-shifted the Soret band and increased the absorption at 460 nm in the first minute (Figure 6A). Subsequently, the spectrum reverted back to that of the resting state ($k^{app} \sim 0.3$ min^{-1}), perhaps as the result of intramolecular electron transfer as reported for myoglobin (Figure 6A).[37] Addition of a further excess (50 equiv) of *m*CPBA to the IsdI–heme complex produced (~1 min) a species with maxima at 404, 458, 578 nm and a shoulder at 605 nm (Figure 6B). This intermediate was not observed in the presence of guaiacol (Figure 5B), suggesting that this species is a ferryl form of the protein. However, the spectrum obtained for this intermediate did not resemble that of ferryl species reported for other heme proteins, an observation that may be attributable to the heme ruffling that is characteristic of IsdI. The ferryl intermediate resulting from reaction of the IsdI–heme complex with excess *m*CPBA partially reverted back to the resting state over 7 min ($k^{app} \sim 0.44$ min^{-1}), and then all absorption maxima started to decrease (Figure 6C) ($k^{app} \sim 0.02$ min^{-1}).

HPLC and LC-MS analysis of these reaction mixtures demonstrated that the major product of reaction with *m*CPBA was unmodified heme (Figure 7B,C). The retention times of heme observed in these reaction mixtures were slightly shifted compared to that for the unreacted IsdI–heme complex, likely because of a change in the oxidation state (Figure 7). A minor

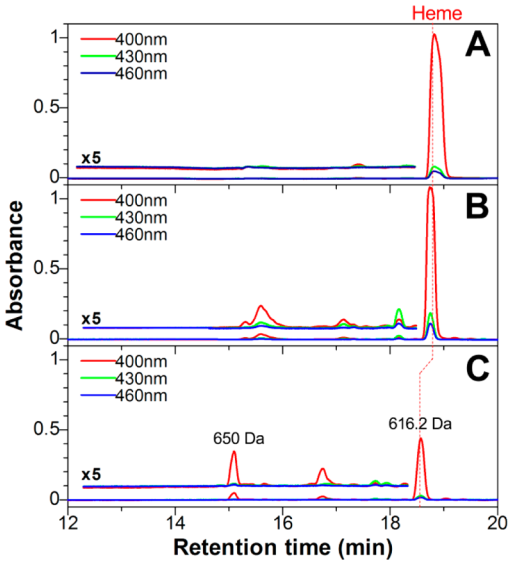

Figure 7. HPLC traces of *m*CPBA reaction products separated with a linear acetonitrile gradient. The IsdI–heme complex (100 μM) was reacted with (A) 0 μM, (B) 500 μM, or (C) 5 mM *m*CPBA. Masses obtained by LC-MS for two distinct peaks observed in panel C are indicated.

peak eluting at ~15 min was observed in the HPLC analysis of the *m*CPBA (50 equiv) reaction products (Figure 7C). The mass of this species was 650 Da, which corresponds to heme with the addition of two OH groups. A similar product was reported for the reaction of myoglobin with H_2O_2 in which two OH groups were added to the heme *β-meso*.[38] Nevertheless, this minor byproduct is not likely to be related to intermediates in the native reaction of IsdI. Addition of ascorbic acid after reaction with *m*CPBA (5 equiv) produced staphylobilins (Figure 8B) at approximately half the yield resulting from the reaction without *m*CPBA (Figure 8A). Furthermore, this low yield is obtained even though electronic absorption spectra indicate that most of the protein returned to the original oxidation state (Figure 6A). Addition of ascorbate following reaction of the IsdI–heme complex with *m*CPBA (50 equiv) produced a minimal yield of staphylobilins (Figure 8C).

DFT Calculation Study. The first step of heme oxidation by HO was initially believed to occur in a concerted manner in which O–O bond cleavage and O–C (*α-meso*) bond formation occur simultaneously.[39] However, independent DFT calculations of the canonical HO reaction reported by Kamachi et al.[40] and Sharma et al.[41] both concluded that the energy barrier of the concerted reaction is too great (40–46 kcal/mol) for this mechanism to proceed under physiological conditions. There-

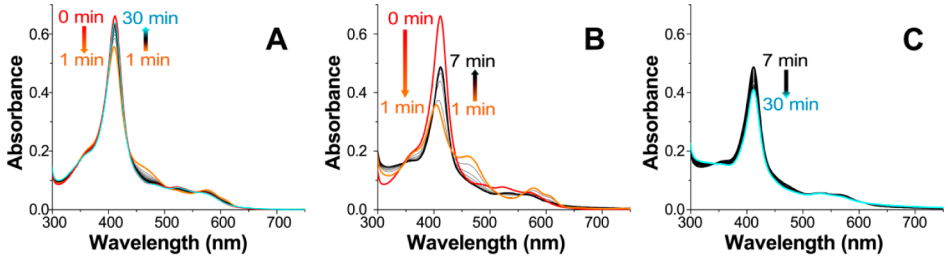

Figure 6. (A) Reaction of the IsdI–heme complex (10 μM) with *m*CPBA (50 μM). Electronic spectra were recorded at 1 min intervals: red for 0 min, orange for 1 min, and blue for 30 min. (B and C) Reaction of the IsdI–heme complex (10 μM) with *m*CPBA (500 μM): red for 0 min, orange for 1 min, and blue for 30 min.

DOI: 10.1021/acs.biochem.5b00239
Biochemistry 2015, 54, 2613–2621

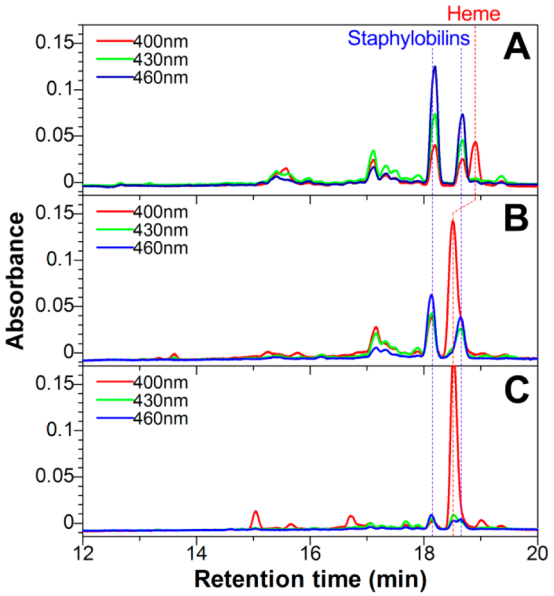

Figure 8. HPLC traces of the products resulting from two-step reactions. The IsdI–heme complex (100 μM) was reacted with (A) 0 μM, (B) 500 μM, or (C) 5 mM *m*CPBA followed by ascorbate (2 mM).

fore, two alternate mechanisms were proposed: a water-assisted oxo mechanism[42,43] and a stepwise radical mechanism.[41,44,45] In both mechanisms, a water cluster present in the active site plays a crucial role in directing an oxidizing species to the porphyrin ring.

No analogous water cluster or other potential hydrogen donor occurs at the active site of IsdI, so an HO-like mechanism seems unlikely. For this reason, the energetic consequences of heme ruffling, characteristic of heme bound to IsdI, on a concerted reaction mechanism were evaluated by DFT calculations. Ruffling of heme can be defined by the C_α–N–N–C_α dihedral angle as shown in Scheme 1A. Four such

Scheme 1. (A) Definition of Dihedral Angle That Provides a Measure of Porphyrin Ruffling and (B) Four Ruffling Dihedral Angles That Can Occur in One Porphyrin Ring

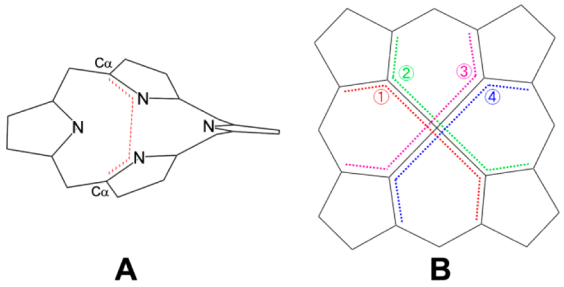

angles can be obtained for one heme (Scheme 1B), and the average value of these angles from the crystal structure of the IsdI–heme complex (PDB entry 3LGN) is 41.6°. In the calculations presented here, we constrained all four ruffling dihedral angles of porphine to be at least 40°. Figure 9 compares the energy profiles resulting from calculations for a concerted reaction mechanism that assumes involvement of a either a planar or a ruffled Fe(III)–OOH intermediate. For a planar intermediate, the activation energy of the reaction was 46.9 kcal/mol, which is in agreement with those of previous

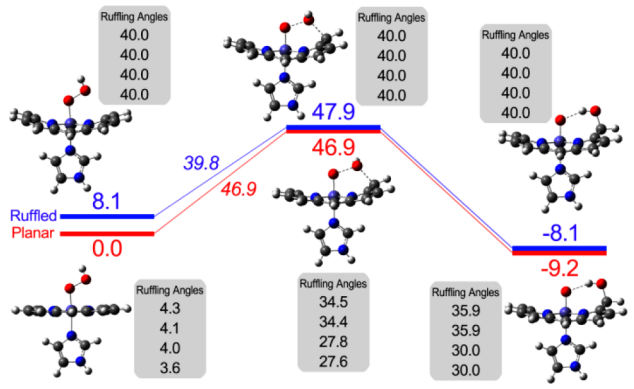

Figure 9. Energy profile (in kilocalories per mole) for the concerted heme oxidation reaction involving planar (red) and ruffled (blue) Fe(III)–OOH intermediates. Energy values are relative to the reactant of the planar structure. The activation energies of the reaction and porphyrin ruffling dihedral angles of each structure are also indicated.

studies (Figure 9).[40,41] One reason for such a high activation energy is that the concerted mechanism requires the porphyrin ring to be significantly distorted at the transition state [35° for two dihedral angles (Figure 9)]. Consequently, if the heme conformation is ruffled in the resting state, the energy barrier for reaction is expected to be lowered. Indeed, the activation energy of the reaction for the ruffled model was 7 kcal/mol lower than that predicted for the planar model. Nevertheless, the barrier was still too great (39.8 kcal/mol) for the reaction to proceed readily by this mechanism under physiological conditions (Figure 9).

Similar calculations for a concerted mechanism mediated by a planar Fe(III)–OO^- intermediate lowered the activation barrier to 21.3 kcal/mol, but the product of this (endoergic) reaction was 6.0 kcal/mol greater than that of the reactant. On the other hand, calculations for the same mechanism involving a ruffled Fe(III)–OO^- intermediate lowered the activation energy to 12.6 kcal/mol (Figure 10) and lowered the difference in energy between the reactant and product to 1.5 kcal/mol, so this latter combination of mechanism and intermediate is energetically more favorable (Figure 10). Ultimately, the overall reaction is expected to be exothermic and to result in the

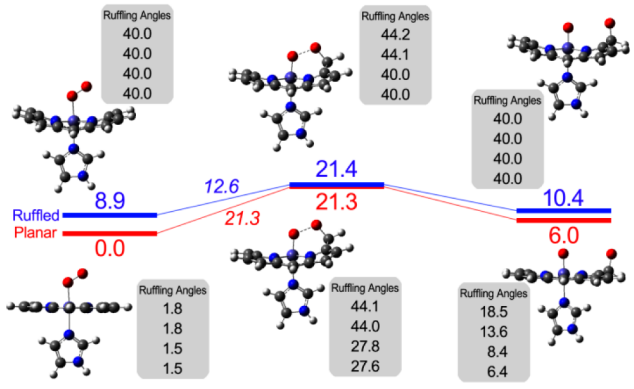

Figure 10. Energy profile (in kilocalories per mole) for the concerted heme oxidation reaction involving planar (red) and ruffled (blue) Fe(III)–OO^- intermediates. Energy values are relative to the reactant of the planar structure. The activation energies of the reaction and porphyrin ruffling dihedral angles of each structure are also indicated.

DOI: 10.1021/acs.biochem.5b00239
Biochemistry 2015, 54, 2613–2621

formation of hydroxyheme or another unidentified IsdI reaction intermediate.[40]

DISCUSSION

Recent identification of the proton source for compound I of cytochrome *c* peroxidase highlights progress made in several laboratories in the structural characterization of reactive iron-centered oxidative intermediates formed at the active sites of oxidative heme enzymes through application of both physical and theoretical methods.[26,46] The active sites of these heme enzymes have evolved structural features that favor the formation of distinct oxygen species for catalysis of specific reactions. These intermediates include ferryl [Fe(IV)=O], peroxo [Fe(III)−OO^-], hydroperoxo [Fe(III)−OOH], or oxygenated [Fe(II)−O_2 or Fe(III)−O_2^-] states of heme iron that form as the result of reaction with dioxygen or peroxide and in some cases a reductant. In addition, the proton or hydrogen sources required for protonation of the relevant coordinated form of oxygen or for subsequent steps in catalysis have been identified for some of these heme enzymes. Heme oxidation is unusual in that the heme is both a cofactor and substrate of the enzyme. Oxidation of heme by IsdI provides an intriguing example of a mechanism in which distortion of the heme substrate/cofactor structure by the active site allows catalysis. The proposed intermediate [Fe(III)−OO^-] would otherwise be incapable of promoting reaction because of the lack of a source of protons to form the more reactive Fe(III)−OOH intermediate that is characteristic of the canonical HOs. The evidence demonstrating the linkage between distortion of the heme substrate and the involvement of an oxidative Fe(III)−OO^- intermediate is summarized below.

The Initial Reactive Species of IsdI and Canonical HOs Are Inequivalent. The initial reaction step of HO has been studied extensively.[47,48] *In vivo*, resting state ferric HO accepts two electrons from P450 reductase/NADPH to form an Fe(III)−OO^- species. Subsequently, one proton is proposed to be rapidly delivered from a distal water cluster molecule to form the Fe(III)−OOH intermediate. Protonation of the Fe(III)−OO^- species is sufficiently efficient that cryoreduction of HO at 77 K resulted in the direct formation of the Fe(III)−OOH species.[49] This Fe(III)−OOH intermediate can hydroxylate the heme to yield *α-meso*-hydroxyheme at higher temperatures.[39,49] Alternatively, the Fe(III)−OOH intermediate can be obtained directly from the resting state by addition of H_2O_2, a process called the "peroxide shunt". The reaction of H_2O_2 (1 equiv) with HO-heme produces verdoheme, and subsequent addition of an electron results in the formation of biliverdin, the native heme oxidation product of HO.[35] However, the IsdI−heme complex is less reactive toward H_2O_2 as addition of 1 or 5 equiv of H_2O_2 produced no specific intermediate (Figures 2 and 3). Consequently, addition of ascorbic acid after the H_2O_2 reaction did not lead to staphylobilin formation (Figure 4). These results do not support the hypothesis that the initial step in heme oxidation by IsdI involves an Fe(III)−OOH species.

Theoretical studies suggested that the water cluster at the actives site of HO is required not only for donation of a proton to the Fe(III)−OO^- species but also for the reaction mechanism of the enzyme. Calculations by Kamachi et al.[42,43] showed that a water-assisted oxo mechanism requires much less activation energy (18 kcal/mol) than the concerted mechanism. Shaik and co-workers proposed an alternative mechanism, called the stepwise radical mechanism, in which an OH radical is produced initially and then attacks the porphyrin ring.[41,44,45] This mechanism also has a small activation energy (−20 kcal/mol), and the water cluster is proposed to play a crucial role in directing the highly reactive OH radical to the *meso* position. However, these two mechanisms are not likely to be applicable to IsdI because no water cluster is observed in the distal heme pocket of this protein.[18]

In contrast to a planar HO-bound heme, X-ray crystallography studies have shown that heme bound to IsdI has a unique ruffled conformation.[15,18,19] This ruffling is proposed to be essential for catalysis, and active site amino acid variants with a decreased level of heme ruffling exhibit reduced heme degradation activity.[19] Our calculations for a concerted mechanism with a model of a ruffled Fe(III)−OOH heme intermediate resulted in an energy barrier (39.8 kcal/mol) that is lower than that predicted for a planar Fe(III)−OOH intermediate (46.9 kcal/mol), but the magnitude of this barrier nevertheless indicates that such an intermediate is not likely to be involved under physiological conditions (Figure 9). This prediction is consistent with our spectroscopic and HPLC studies of reactions of the IsdI−heme complex with H_2O_2 that did not produce intermediates leading to the staphylobilins. Our observation that the reaction of the IsdI−heme complex with H_2O_2 resulted in the random destruction of heme may be related to a stepwise radical mechanism insofar as production of an OH radical upon addition of H_2O_2 to the IsdI−heme complex may result in indiscriminate attack on the heme.

A Ferryl Intermediate Is Not the Initial Reactive Species of IsdI. The electron-withdrawing acyl group in *m*CPBA facilitates O−O bond heterolysis and leads to the formation of ferryl species when the acyl group is added to heme proteins.[23] The production of ferryl species following reaction of this reagent with the IsdI−heme complex was confirmed by the increase in absorption around 470 nm in the presence of excess guaiacol (Figure 5B). The ferryl heme−IsdI complex was stable and exhibited a unique absorption spectrum that probably results from the heme ruffling observed in IsdI (Figure 6B). The stability of the IsdI ferryl species implies it is not active in heme degradation, and instead, the enzyme appeared to autoreduce gradually to the Fe(III)−OH resting state (Figure 6A,B). Similar autoreduction of ferryl heme was reported for myoglobin, and Tyr and Trp residues were identified as electron donors in this process.[37] IsdI has a Trp residue (Trp66) in the vicinity of the heme that may be required for autoreduction of ferryl heme in this protein. Excess *m*CPBA could overcome the autoreduction reaction and lead to random heme destruction (Figure 7). Nonetheless, HPLC and LC-MS analyses indicated that some of the heme remained intact even after reaction with a 50-fold excess of *m*CPBA (Figure 7C). However, once the IsdI−heme complex had been converted to a ferryl species, the native heme oxidizing function was perturbed, and staphylobilins were not produced in the presence of ascorbic acid (Figure 8). Similarly, the reaction of *m*CPBA with HO is known to produce a compound II-like intermediate that does not oxidize heme to verdoheme.[35]

Evidence of an Fe(III)−OO^- Intermediate as the Initial Reactive Species of IsdI. The lack of evidence for either an Fe(III)−OOH or a ferryl intermediate in the initial reaction of IsdI suggests that an Fe(III)−OO^- species is relevant to the IsdI catalytic cycle. This hypothesis is supported by crystallographic structures of the IsdI−heme complex that lack an observed water cluster or a protein group situated to deliver a proton to an oxygen species bound to the heme iron. Precedence for a catalytically relevant Fe(III)−OO^- species is

DOI: 10.1021/acs.biochem.5b00239
Biochemistry 2015, 54, 2613−2621

found in some cytochromes P450, e.g., CYP17,[28] CYP19,[29] CYP51,[30] and CYP125.[31] Also, nitric oxide synthase is proposed to use an Fe(III)−OO^- intermediate to catalyze the nucleophilic addition of oxygen to a carbon−nitrogen double bond.[50] The Fe(III)−OO^- species is more electron rich than the Fe(III)−OOH species, so it is more suitable for a nucleophilic addition reaction.

The involvement of an Fe(III)−OO^- species correlates well with the electron configuration of heme iron bound to IsdI.[51] ^{1}H NMR spectra of the IsdI−heme cyanide complex exhibited an unprecedented shift of the heme *meso*-H signals more than 10 ppm upfield. This shift can be explained by the iron of a ruffled heme exhibiting the uncommon $(d_{xz},d_{yz})^4(d_{xy})^1$ electron configuration that would decrease the electron density at the *meso* positions and render them more susceptible to nucleophilic attack. Moreover, the ruffling of the heme orients the *β*- and *δ*-*meso*-carbon positions to favor attack from a peroxoanion bound to the iron.[18]

Our theoretical study showed that a concerted heme oxidation mechanism with an Fe(III)−OO^- intermediate is energetically accessible [21.3 and 12.6 kcal/mol for planar and ruffled heme models, respectively (Figure 10)]. The activation energy was modest for both ruffled and planar heme models, and in both IsdI and HO, the Fe(III)−OO^- species is likely part of the reaction pathway. With HO, this species is rapidly protonated to an Fe(III)−OOH intermediate prior to reaction with the heme.[49] Other heme-based oxygenases such as CYP101 (P450cam),[52] CYP2B4,[53] nitric oxide synthase,[54] and CYP119[55] are also known to form Fe(III)−OOH species based on cryoreduction experiments at 77 K. On the other hand, CYP19 produces the Fe(III)−OO^- species rather than the Fe(III)−OOH species after cryoreduction, and this enzyme is proposed to employ the Fe(III)−OO^- species as a reactive species in a reaction step.[29] For the initial reaction step, IsdI has no obvious proton-donating group in its distal site,[18] so the Fe(III)−OO^- species is expected to be favored, as well. A concerted heme oxidation mechanism involving an Fe(III)−OO^- intermediate requires a large degree of heme distortion in the transition state (Figure 10). While heme distortion of such magnitude is unlikely to occur in most heme proteins, the active site of IsdI clearly promotes such heme ruffling (Figure 11).

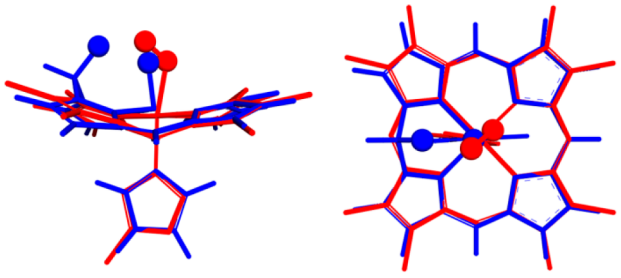

Figure 11. Superimposed structures of the heme active site in IsdI (PDB entry 3LGN, red) and calculated transition state structure of the Fe(III)−OO^- concerted mechanism (blue). Heme propionate and vinyl groups and His main chain atoms were omitted from the native protein structure. Oxygen atoms are presented as spheres, and other atoms are drawn as sticks.

AUTHOR INFORMATION

Corresponding Author

*Department of Microbiology and Immunology, University of British Columbia, Vancouver, BC, Canada. Telephone: 604-822-8022. E-mail: michael.murphy@ubc.ca.

Author Contributions

S.-i.J.T. and S.A.L. contributed equally to this work.

Funding

This work was supported by a grant from Canadian Institutes of Health Research (MOP-49597) to M.E.P.M., a Canada Research Chair (A.G.M.), and the Canadian Foundation for Innovation (to A.G.M. and M.E.P.M.). S.A.L. was supported by a Natural Sciences and Engineering Research Council of Canada postdoctoral fellowship.

Notes

The authors declare no competing financial interest.

ACKNOWLEDGMENTS

We thank Dr. Emily Seo, director of the UBC Department of Chemistry Shared Instrument Facility, for access to ESI-MS equipment.

ABBREVIATIONS

HO, heme oxygenase; DFT, density functional theory; *m*CPBA, *m*-chloroperoxybenzoic acid; PDB, Protein Data Bank.

REFERENCES

(1) Ratledge, C., and Dover, L. G. (2000) Iron metabolism in pathogenic bacteria. *Annu. Rev. Microbiol. 54*, 881−941.

(2) Thurlow, L. R., Joshi, G. S., and Richardson, A. R. (2012) Virulence strategies of the dominant USA300 lineage of community-associated methicillin-resistant *Staphylococcus aureus* (CA-MRSA). *FEMS Immunol. Med. Microbiol. 65*, 5−22.

(3) Hammer, N. D., and Skaar, E. P. (2011) Molecular mechanisms of *Staphylococcus aureus* iron acquisition. *Annu. Rev. Microbiol. 65*, 129−147.

(4) Skaar, E. P., Gaspar, A. H., and Schneewind, O. (2004) IsdG and IsdI, heme-degrading enzymes in the cytoplasm of *Staphylococcus aureus*. *J. Biol. Chem. 279*, 436−443.

(5) Tenhunen, R., Marver, H., Pimstone, N. R., Trager, W. F., Cooper, D. Y., and Schmid, R. (1972) Enzymatic degradation of heme. Oxygenative cleavage requiring cytochrome P-450. *Biochemistry 11*, 1716−1720.

(6) Wilks, A., and Ortiz de Montellano, P. R. (1993) Rat liver heme oxygenase. High level expression of a truncated soluble form and nature of the *meso*-hydroxylating species. *J. Biol. Chem. 268*, 22357−22362.

(7) Wilks, A., Torpey, J., and Ortiz de Montellano, P. R. (1994) Heme oxygenase (HO-1). Evidence for electrophilic oxygen addition to the porphyrin ring in the formation of *α*-*meso*-hydroxyheme. *J. Biol. Chem. 269*, 29553−29556.

(8) Liu, Y., Moenne-Loccoz, P., Loehr, T. M., and Ortiz de Montellano, P. R. (1997) Heme oxygenase-1, intermediates in verdoheme formation and the requirement for reduction equivalents. *J. Biol. Chem. 272*, 6909−6917.

(9) Chu, G. C., Katakura, K., Zhang, X., Yoshida, T., and Ikeda-Saito, M. (1999) Heme degradation as catalyzed by a recombinant bacterial heme oxygenase (Hmu O) from *Corynebacterium diphtheriae*. *J. Biol. Chem. 274*, 21319−21325.

(10) Tenhunen, R., Marver, H. S., and Schmid, R. (1969) Microsomal heme oxygenase: Characterization of the enzyme. *J. Biol. Chem. 244*, 6388−6394.

(11) Unno, M., Matsui, T., Chu, G. C., Couture, M., Yoshida, T., Rousseau, D. L., Olson, J. S., and Ikeda-Saito, M. (2004) Crystal structure of the dioxygen-bound heme oxygenase from *Corynebacte-*

DOI: 10.1021/acs.biochem.5b00239
Biochemistry 2015, 54, 2613−2621

rium diphtheriae: Implications for heme oxygenase function. *J. Biol. Chem. 279*, 21055−21061.
(12) Matsui, T., Furukawa, M., Unno, M., Tomita, T., and Ikeda-Saito, M. (2005) Roles of distal Asp in heme oxygenase from *Corynebacterium diphtheriae*, HmuO: A water-driven oxygen activation mechanism. *J. Biol. Chem. 280*, 2981−2989.
(13) Davydov, R., Kofman, V., Fujii, H., Yoshida, T., Ikeda-Saito, M., and Hoffman, B. M. (2002) Catalytic mechanism of heme oxygenase through EPR and ENDOR of cryoreduced oxy-heme oxygenase and its Asp 140 mutants. *J. Am. Chem. Soc. 124*, 1798−1808.
(14) Davydov, R., Matsui, T., Fujii, H., Ikeda-Saito, M., and Hoffman, B. M. (2003) Kinetic isotope effects on the rate-limiting step of heme oxygenase catalysis indicate concerted proton transfer/heme hydroxylation. *J. Am. Chem. Soc. 125*, 16208−16209.
(15) Reniere, M. L., Ukpabi, G. N., Harry, S. R., Stec, D. F., Krull, R., Wright, D. W., Bachmann, B. O., Murphy, M. E., and Skaar, E. P. (2010) The IsdG-family of haem oxygenases degrades haem to a novel chromophore. *Mol. Microbiol. 75*, 1529−1538.
(16) Matsui, T., Nambu, S., Ono, Y., Goulding, C. W., Tsumoto, K., and Ikeda-Saito, M. (2013) Heme degradation by *Staphylococcus aureus* IsdG and IsdI liberates formaldehyde rather than carbon monoxide. *Biochemistry 52*, 3025−3027.
(17) Loutet, S. A., Kobylarz, M. J., Chau, C. H. T., and Murphy, M. E. P. (2013) IruO is a reductase for heme degradation by IsdI and IsdG in *Staphylococcus aureus*. *J. Biol. Chem. 288*, 25749−25759.
(18) Lee, W. C., Reniere, M. L., Skaar, E. P., and Murphy, M. E. P. (2008) Ruffling of metalloporphyrins bound to IsdG and IsdI, two heme-degrading enzymes in *Staphylococcus aureus*. *J. Biol. Chem. 283*, 30957−30963.
(19) Ukpabi, G., Takayama, S.-i. J., Mauk, A. G., and Murphy, M. E. P. (2012) Inactivation of IsdI heme oxidation by an active site substitution that diminishes heme ruffling. *J. Biol. Chem. 287*, 34179−34188.
(20) Schuller, D. J., Wilks, A., Ortiz de Montellano, P. R., and Poulos, T. L. (1999) Crystal structure of human heme oxygenase-1. *Nat. Struct. Biol. 6*, 860−867.
(21) Schuller, D. J., Zhu, W., Stojiljkovic, I., Wilks, A., and Poulos, T. L. (2001) Crystal structure of heme oxygenase from the Gram-negative pathogen *Neisseria meningitidis* and a comparison with mammalian heme oxygenase-1. *Biochemistry 40*, 11552−11558.
(22) Hirotsu, S., Chu, G. C., Unno, M., Lee, D. S., Yoshida, T., Park, S. Y., Shiro, Y., and Ikeda-Saito, M. (2004) The crystal structures of the ferric and ferrous forms of the heme complex of HmuO, a heme oxygenase of *Corynebacterium diphtheriae*. *J. Biol. Chem. 279*, 11937−11947.
(23) Groves, J. T., and Watanabe, Y. (1988) Reactive iron porphyrin derivatives related to the catalytic cycles of cytochrome P-450 and peroxidase. Studies of the mechanism of oxygen activation. *J. Am. Chem. Soc. 110*, 8443−8452.
(24) Behan, R. K., and Green, M. T. (2006) On the status of ferryl protonation. *J. Inorg. Biochem. 100*, 448−459.
(25) Behan, R. K., Hoffart, L. M., Stone, K. L., Krebs, C., and Green, M. T. (2006) Evidence for basic ferryls in cytochromes P450. *J. Am. Chem. Soc. 128*, 11471−11474.
(26) Casadei, C. M., Gumiero, A., Metcalfe, C. L., Murphy, E. J., Basran, J., Concilio, M. G., Teixeira, S. C., Schrader, T. E., Fielding, A. J., Ostermann, A., Blakeley, M. P., Raven, E. L., and Moody, P. C. (2014) Neutron cryo-crystallography captures the protonation state of ferryl heme in a peroxidase. *Science 345*, 193−197.
(27) Gumiero, A., Metcalfe, C. L., Pearson, A. R., Raven, E. L., and Moody, P. C. E. (2011) Nature of the ferryl heme in compounds I and II. *J. Biol. Chem. 286*, 1260−1268.
(28) Lee-Robichaud, P., Akhtar, M. E., Wright, J. N., Sheikh, Q. I., and Akhtar, M. (2004) The cationic charges on Arg347, Arg358 and Arg449 of human cytochrome P450c17 (CYP17) are essential for the enzyme's cytochrome b_5-dependent acyl-carbon cleavage activities. *J. Steroid Biochem. Mol. Biol. 92*, 119−130.
(29) Gantt, S. L., Denisov, I. G., Grinkova, Y. V., and Sligar, S. G. (2009) The critical iron−oxygen intermediate in human aromatase. *Biochem. Biophys. Res. Commun. 387*, 169−173.
(30) Sen, K., and Hackett, J. C. (2010) Peroxo−iron mediated deformylation in sterol 14α-demethylasecatalysis. *J. Am. Chem. Soc. 132*, 10293−10305.
(31) Sivaramakrishnan, S., Ouellet, H., Matsumura, H., Guan, S., Moënne-Loccoz, P., Burlingame, A. L., and Ortiz de Montellano, P. R. (2012) Proximal ligand electron donation and reactivity of the cytochrome P450 ferric−peroxo anion. *J. Am. Chem. Soc. 134*, 6673−6684.
(32) Chung, L. W., Li, X., Sugimoto, H., Shiro, Y., and Morokuma, K. (2010) ONIOM study on a missing piece in our understanding of heme chemistry: Bacterial tryptophan 2,3-dioxygenase with dual oxidants. *J. Am. Chem. Soc. 132*, 11993−12005.
(33) Frisch, M. J., Trucks, G. W., Schlegel, H. B., Scuseria, G. E., Robb, M. A., Cheeseman, J. R., Scalmani, G., Barone, V., Mennucci, B., Petersson, G. A., Nakatsuji, H., Caricato, M., Li, X., Hratchian, H. P., Izmaylov, A. F., Bloino, J., Zheng, G., Sonnenberg, J. L., Hada, M., Ehara, M., Toyota, K., Fukuda, R., Hasegawa, J., Ishida, M., Nakajima, T., Honda, Y., Kitao, O., Nakai, H., Vreven, T., Montgomery, J. A., Jr., Peralta, J. E., Ogliaro, F., Bearpark, M., Heyd, J. J., Brothers, E., Kudin, K. N., Staroverov, V. N., Kobayashi, R., Normand, J., Raghavachari, K., Rendell, A., Burant, J. C., Iyengar, S. S., Tomasi, J., Cossi, M., Rega, N., Millam, J. M., Klene, M., Knox, J. E., Cross, J. B., Bakken, V., Adamo, C., Jaramillo, J., Gomperts, R., Stratmann, R. E., Yazyev, O., Austin, A. J., Cammi, R., Pomelli, C., Ochterski, J. W., Martin, R. L., Morokuma, K., Zakrzewski, V. G., Voth, G. A., Salvador, P., Dannenberg, J. J., Dapprich, S., Daniels, A. D., Farkas, Foresman, J. B., Ortiz, J. V., Cioslowski, J., and Fox, D. J. (2009) *Gaussian 09*, revision A.02, Gaussian, Inc., Wallingford, CT.
(34) Wachters, A. J. H. (1970) Gaussian basis set for molecular wavefunctions containing third-row atoms. *J. Chem. Phys. 52*, 1033−1036.
(35) Wilks, A., and Ortiz de Montellano, P. R. (1993) Rat liver heme oxygenase. High level expression of a truncated soluble form and nature of the meso-hydroxylating species. *J. Biol. Chem. 268*, 22357−22362.
(36) Koduri, R. S., and Tien, M. (1995) Oxidation of guaiacol by lignin peroxidase: Role of veratryl alcohol. *J. Biol. Chem. 270*, 22254−22258.
(37) Lardinois, O. M., and Ortiz de Montellano, P. R. (2004) Autoreduction of ferryl myoglobin: Discrimination among the three tyrosine and two tryptophan residues as electron donors. *Biochemistry 43*, 4601−4610.
(38) Sugiyama, K., Highet, R. J., Woods, A., Cotter, R. J., and Osawa, Y. (1997) Hydrogen peroxide-mediated alteration of the heme prosthetic group of metmyoglobin to an iron chlorin product: Evidence for a novel oxidative pathway. *Proc. Natl. Acad. Sci. U.S.A. 94*, 796−801.
(39) Wilks, A., Torpey, J., and Ortiz de Montellano, P. R. (1994) Heme oxygenase (HO-1). Evidence for electrophilic oxygen addition to the porphyrin ring in the formation of α-meso-hydroxyheme. *J. Biol. Chem. 269*, 29553−29556.
(40) Kamachi, T., Shestakov, A. F., and Yoshizawa, K. (2004) How heme metabolism occurs in heme oxygenase: Computational study of oxygen-donation ability of the oxo and hydroperoxo species. *J. Am. Chem. Soc. 126*, 3672−3673.
(41) Sharma, P. K., Kevorkiants, R., de Visser, S. P., Kumar, D., and Shaik, S. (2004) Porphyrin traps its terminator! Concerted and stepwise porphyrin degradation mechanisms induced by heme-oxygenase and cytochrome P450. *Angew. Chem. 43*, 1129−1132.
(42) Kamachi, T., Nishimi, T., and Yoshizawa, K. (2012) A new understanding on how heme metabolism occurs in heme oxygenase: Water-assisted oxo mechanism. *Dalton Trans. 41*, 11642−11650.
(43) Kamachi, T., and Yoshizawa, K. (2005) Water-assisted oxo mechanism for heme metabolism. *J. Am. Chem. Soc. 127*, 10686−10692.

DOI: 10.1021/acs.biochem.5b00239
Biochemistry 2015, 54, 2613−2621

(44) Kumar, D., de Visser, S. P., and Shaik, S. (2005) Theory favors a stepwise mechanism of porphyrin degradation by a ferric hydroperoxide model of the active species of heme oxygenase. *J. Am. Chem. Soc. 127*, 8204−8213.
(45) Chen, H., Moreau, Y., Derat, E., and Shaik, S. (2008) Quantum mechanical/molecular mechanical study of mechanisms of heme degradation by the enzyme hemeoxygenase: The strategic function of the water cluster. *J. Am. Chem. Soc. 130*, 1953−1965.
(46) Groves, J. T., and Boaz, N. C. (2014) Fishing for peroxidase protons. *Science 345*, 142−143.
(47) Sono, M., Roach, M. P., Coulter, E. D., and Dawson, J. H. (1996) Heme-containing oxygenases. *Chem. Rev. 96*, 2841−2888.
(48) Matsui, T., Unno, M., and Ikeda-Saito, M. (2010) Heme oxygenase reveals its strategy for catalyzing three successive oxygenation reactions. *Acc. Chem. Res. 43*, 240−247.
(49) Davydov, R. M., Yoshida, T., Ikeda-Saito, M., and Hoffman, B. M. (1999) Hydroperoxy-heme oxygenase generated by cryoreduction catalyzes the formation of *α-meso*-hydroxyheme as detected by EPR and ENDOR. *J. Am. Chem. Soc. 121*, 10656−10657.
(50) Pufahl, R. A., Wishnok, J. S., and Marletta, M. A. (1995) Hydrogen peroxide-supported oxidation of N^G-hydroxy-L-arginine by nitric oxide synthase. *Biochemistry 34*, 1930−1941.
(51) Takayama, S.-i. J., Ukpabi, G., Murphy, M. E. P., and Mauk, A. G. (2011) Electronic properties of the highly ruffled heme bound to the heme degrading enzyme IsdI. *Proc. Natl. Acad. Sci. U.S.A. 108*, 13071−13076.
(52) Davydov, R., Perera, R., Jin, S., Yang, T.-C., Bryson, T. A., Sono, M., Dawson, J. H., and Hoffman, B. M. (2005) Substrate modulation of the properties and reactivity of the oxy-ferrous and hydroperoxo-ferric intermediates of cytochrome P450cam as shown by cryoreduction-EPR/ENDOR spectroscopy. *J. Am. Chem. Soc. 127*, 1403−1413.
(53) Davydov, R., Razeghifard, R., Im, S.-C., Waskell, L., and Hoffman, B. M. (2008) Characterization of the microsomal cytochrome P450 2B4 O_2-activation intermediates by cryoreduction and electron paramagnetic resonance. *Biochemistry 47*, 9661−9666.
(54) Davydov, R., Sudhamsu, J., Lees, N. S., Crane, B. R., and Hoffman, B. M. (2009) EPR and ENDOR characterization of the reactive intermediates in the generation of NO by cryoreduced oxy-nitric oxide synthase from *Geobacillus stearothermophilus*. *J. Am. Chem. Soc. 131*, 14493−14507.
(55) Denisov, I. G., Hung, S.-C., Weiss, K. E., McLean, M. A., Shiro, Y., Park, S.-Y., Champion, P. M., and Sligar, S. G. (2001) Characterization of the oxygenated intermediate of the thermophilic cytochrome P450 CYP119. *J. Inorg. Biochem. 87*, 215−226.
(56) *The PyMOL Molecular Graphics System*, version 1.7.0.1 (2015) Schrödinger, LLC, Portland, OR.

DOI: 10.1021/acs.biochem.5b00239
Biochemistry 2015, 54, 2613−2621